Online Appendix for "The Time-Varying and Volatile Macroeconomic Effects of Immigration"

Huachen Li*

October 28, 2020

Not intended for publication.

*Assistant Professor of Economics. Department of Economics, Kenyon College, 302 Ascension Hall, 202 College Park St, Gambier, OH 43022. Email: li8@kenyon.edu.

Appendix A. Relevant Recent Changes in U.S. Immigration Policy

This appendix describes eight important immigration policy changes since the 1960s that are relevant to this paper.

1. *The Immigration and Nationality Act of 1965 (the Hart-Celler Act)* was one of the largest changes in U.S. immigration policy during the sample period. The Act replaced the Immigration Act of 1924 which largely restricts non-white immigration. The Act created immigration categories targeting relatives of U.S. citizens and permanent residents which are exempted from the total immigration limits. Although the Act had small effects on the level of immigration, it drastically changed its demographic composition. Law (2002) documents this long-run effect.

2. *The Refugee Act of 1980* provided the first clear definition of refugee immigration to the U.S. and allocated a 50,000 cap on refugee admission with an unlimited cap for certain protocols. Benson (2016) argues that the implication of this policy change is the marking of a wave of open-door policies. Immigration policy fluctuates between being restrictive and permissive, a perception that affects expectation on migration difficulty. Potential immigrants interpret these policy changes differently, which may offer an unintended incentive to migrate (Hanson and Splimbergo 2001; Correa-Cabrera and Rojas-Arenaza 2012).

3. *The Immigration Reform and Control Act (IRCA) of 1986* legalized irregular immigrants since 1982 and created a new class of working visa/visa waiver program. The IRCA was considered the largest nationwide amnesty of irregular immigration in history and a strong signal of an era of nonrestrictive immigration policies (Vernez 1993; Baker 1997; Orrenius and Zavodny 2003). The amnesty was followed by a high level of inflow and employment of immigration in the 1990s.

4. The *American Homecoming Act and the Immigration Act of 1990 (IMMACT)* raised the annual total immigration cap to 790,000 (a 290,000 addition), provided an additional 140,000 visa cap, and granted special status for immigrants of specific countries of origin. Under the 1990 IMMACT, more than 1.5 million immigrants were granted permanent residency with family- and employment-based sponsorship. The 1990 IMMACT also re-categorized employment-based immigration into EB-1 through EB-5 which are still in effect to date. This legislation created the largest increase in immigration cap since 1910. Together with the IRCA, the IMMACT generated the largest inflow of immigration around 1990; See Borjas (1994), Friedberg and Hunt (1995).

5. The enactment of the *Illegal Immigration Reform and Immigrant Responsibility Act of 1996* is a policy reform on irregular immigration[1]. Hanson and Splimbergo (2001) argue that the act was designed to disincentivize irregular immigration by increasing border patrol enforcement, which had a direct effect on the inflow of irregular immigrants.

6. *The American Competitiveness and Workforce Improvement Act of 1998* increased the annual H-1B cap from 65,000 to 115,000 and required employers to pay for H-1B administration fees and worker benefits in accordance with the same criteria as U.S. workers.

7. *The H-1B Visa Reform Act of 2004* reduced the H-1B cap from 195,000 to 65,000 and altered the filing structure.

8. Operation Streamline was the largest operation of aggressive enforcement against unauthorized border-crossing to date. Operation Streamline adopted a zero-tolerance policy in the prosecution and deportation of irregular immigration. According to the DHS, the operation resulted in deportation of 1.54 million immigrants from 2007

[1]The Act lifted the trigger for immediate deportation, announced the right to detain deportees in American jails no less than two years at deportees' expense, and removed the pardon waiver right for unlawful immigrant for a given period of stay in the country.

to 2011. Data on permanent immigration shows a number of consecutive negative spikes post 2005, matching the development and expansion period of Operation Streamline.

Appendix B. Data

B.1. Interpolation of Quarterly Immigration

Interpolation is useful in mitigating the over-fitting problems of a large parameter space from estimating structural SVARs with time-variation. This section describes the interpolation of the immigration series. I adopt the method of Silva and Cardoso (2001) which is a flexible version of the regression based interpolation following Chow and Lin (1971). I compare interpolation results from four popular methods. I show they do not have meaningful differences for the immigration series.

Chow and Lin (1971) develop a best linear unbiased regression interpolation method to estimate high frequency series by running a Generalized Least Squares (GLS) regression using multiple "indicator" series. They assume the regression relationship

$$Y^q = X\beta + \mu,$$

where Y^q is $4n \times 1$ high frequency data of estimation, X is a $4n{\times}p$ matrix that contains p "indicator" series of high frequency, and μ is a random vector with mean zero and variance-covariance matrix V^y. The low frequency (observed) data regression relationship is

$$Y^y = C'X\beta + C'\mu, \tag{B.1}$$

where C is a $n \times 4n$ frequency converter matrix that converts annual series Y^y to quarterly series Y^q. Note that equation B.1 implies that the high frequency variance-covariance matrix, denoted V^q, is equal to the low frequency variance-covariance matrix, V^y, pre and post-multiplying matrix C (i.e. $V^q = CV^yC'$).

Matrix manipulation yields the estimated coefficients

$$\hat{\beta} = [X'C(C'V^yC)^{-1}C'X]^{-1}X'C(C'V^yC)^{-1}Y^y, \tag{B.2}$$

where solving equation B.2 requires knowledge of V^y. The Chow-Lin method defines random variable μ as an AR(1) process. A few extensions of the Chow-Lin method have been done in aim to enhance the interpolation performance. Fernandez (1981) uses a random walk μ for interpolation in order to account for potential non-stationarity and/or serial correlation in the data. Litterman (1983) claims that Fernandez' treatment on data serial correlation fails to remove all serial correlation in certain data series. Litterman's improvement, labeled "Markov random walk", treats μ as an ARIMA(1,1,0). According to Litterman, the mean squared error could be reduced by up to 13%.

I use the Silva and Cardoso (2001), SSC henceforth, approach to interpolate the immigration data from annual to quarterly frequency. The advantage of SSC's model is the autoregressive term in the interpolation

$$Y_t^q = \kappa Y_{t-1}^q + X_t\beta + \mu_t, \tag{B.3}$$

which allows the model to account for cointegration.[2] Parameter κ is numerically estimated to maximize the log-likelihood function of the model. After the optimal κ is set, the following estimation is similar to that of Chow-Lin and its extensions.

Table B.1: SSC Interpolation Statistics

Variable Name	Estimated Beta	St. Dev.	Long Run Effect $\hat{\beta}/(1-\hat{\kappa})$
Income	0.7930	3.6714	4.6645
Civilian Labor Force	0.6879	1.0831	4.0464
Household Survey Pop.	-0.3754	0.6944	-2.2083
Number of Payrolls	0.1602	0.6872	0.9422

Note: $\hat{\kappa}$ = 0.83. The long run effect ($\frac{\hat{\beta}}{1-\hat{\kappa}}$) is equivalent of Chow-Lin regression coefficient.

Using (B.2) and (B.3), Y_t^y is a 80×1 vector of the annual DHS immigration data from 1953 to 2017.[3] X_t is a 260×4 matrix containing real disposable income, civilian labor force, employment household survey population, and number of non-farm pay rolls from

[2] Note that the SSC model is equivalent to that of Fernandez when $\kappa = 1$.

[3] $Y_t^q = Y_t^y C$ where C is the same frequency converting matrix from Chow-Lin.

1953Q1 to 2017Q4. Income provides a benchmark on the macroeconomic connection of immigration, while civilian labor force, household survey, and establishment survey population measure population change from three different perspectives. Table B.1 provides interpolation statistics. The beta coefficients are interpreted as an estimated short-run (1 period lag) sensitivity measure of the indicator series to immigration. The autoregressive coefficient $\hat{\kappa}$ is 0.83, indicating a stationary AR(1) given the SSC model. The estimated long-run effect of the indicator variables (equivalent to the interpretation of β in the Chow-Lin method), given by $\hat{\beta}/(1-\hat{\kappa})$, are presented in column 3.

B.2. Results of Alternative Interpolation Methods

Fig. B.1. Comparison of interpolation methods.

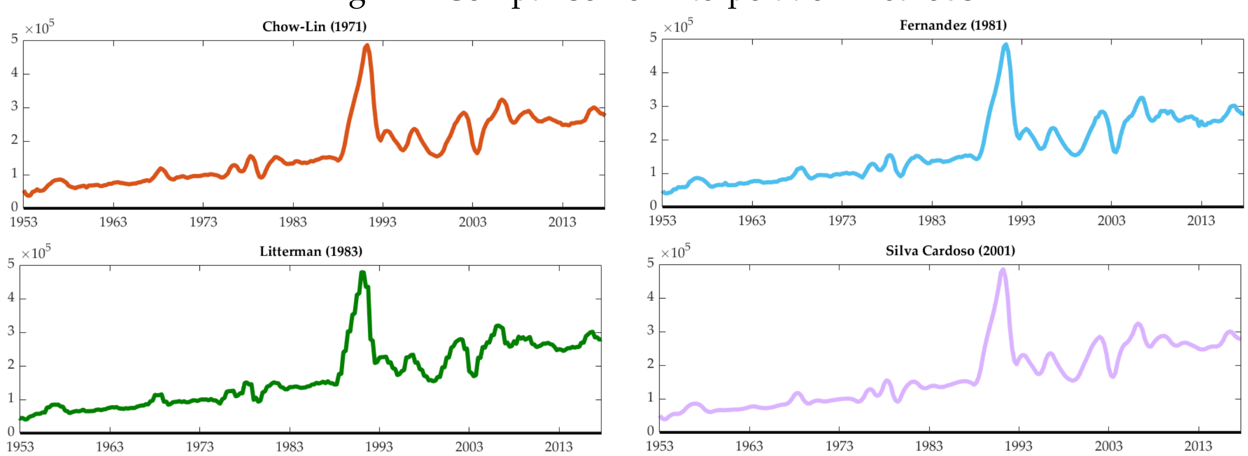

Notes: Sample is 1953Q1 to 2017Q4. Each interpolation result is based on a set of benchmark variables including real disposable income, civilian labor force, employment household survey population, and non-farm payrolls.

Figure B.1 displays a comparison of different interpolation methods considered in the construction of quarterly immigration data. The four regression-based interpolation methods produce highly similar results. Although this paper uses the series estimated by the method of Silva and Cardoso (2001), using other interpolation methods does not alter the main results qualitatively.

B.3. Unit Root Test Results

According to Table B.2, I fail to reject the existence of a unit root in immigration in log levels but rejects the same null at 1% confidence when immigration is in growth rates.

Table B.2: Augmented Dickey-Fuller Test for Unit Root

	Test Statistic	p-value
Immigration in Log Levels	-2.528	0.3141
Immigration in Growth Rates	-4.056	0.0073

Notes: The Dickey-Fuller tests for the null that the immigration series has a unit root. The p-value corresponds to the MacKinnon approximation of the p-value based on the test statistic.

B.4. Data Construction and Sources

Utilization-adjusted average labor productivity data is obtained from the Federal Reserve of San Francisco website following Basu et al. (2006). Series on hours worked come from Cociuba et al. (2018).

To construct consumption in non-durables and services, I obtain the following series reported by the Bureau of Economic Analysis: Per Capita Personal Consumption Expenditure (PCE) in non-durables (c^n), Per Capita PCE series in services (c^s) from NIPA Table 1.1.5, and their corresponding price indexes (p^n, p^s) from NIPA Table 1.1.4. The growth of real PCE in non-durables and services is calculated as a Fisher ideal index (Fisher 1922),

$$c_t = \sqrt{\frac{c_t^n p_t^n + c_t^s p_t^s}{c_{t-1}^n p_t^n + c_{t-1}^s p_t^s} \times \frac{c_t^n p_{t-1}^n + c_t^s p_{t-1}^s}{c_{t-1}^n p_{t-1}^n + c_{t-1}^s p_{t-1}^s}} - 1, \tag{B.4}$$

to correctly account for the addition of chained aggregated NIPA data as suggested by Whelan (2002).

Appendix C. Identification: Details and Robustness

C.1. Galí (1999) Structural VAR

In this appendix, I briefly outline the fixed-parameter bivariate SVAR of Galí (1999) that the baseline SVARs begin with.

Reduced-form VAR

Consider a standard reduced-form VAR with p lags:

$$z_t = \sum_{i=1}^{p} B_i z_{t-i} + e_t, \quad e_t \sim (0_{2\times 1}, \Omega_{2\times 2}), \tag{C.1}$$

where

$$z_t = \begin{bmatrix} \Delta ln(x_t) \\ \Delta ln(n_t) \end{bmatrix},$$

B_i are 2×2 coefficient matrices, for $i = 1...p$, and e_t is a 2×1 reduced-form error term. Vector z_t contains data on ALP (x) and hours worked (n).

The reduced-form VMA(∞) of (C.1) is

$$z_t = [I_2 - B(L)]^{-1} e_t \equiv \Lambda(L) e_t, \tag{C.2}$$

where L is the lag operator and $\Lambda(L)$ denotes the coefficient matrices of the reduced-form error terms.

SVAR and Identification

Imposing long-run neutrality on ALP in the reduced-form VAR of (C.1), the SVAR(p) becomes:

$$z_t = \Gamma(L)\epsilon_t, \quad \Gamma(L) = \sum_{j=0}^{\infty} \Gamma_j L^j, \quad \Gamma_j = \begin{bmatrix} \gamma_{11,j} & \gamma_{12,j} \\ \gamma_{21,j} & \gamma_{22,j} \end{bmatrix}. \tag{C.3}$$

Galí calls the first innovation the TFP shock and the second element the demand shock. He assumes that only a TFP shock has a permanent effect on the level of labor productivity. Economic motivation for this long-run neutrality assumption is discussed in Section II.A of Galí (1999). The cumulative effect of the demand shock on ALP is zero, or

$$\Gamma_{12} = \sum_{j=0}^{\infty} \gamma_{12,j} = 0. \tag{C.4}$$

Hence, the long-run cumulative impact matrix is

$$\Gamma(1) = \begin{bmatrix} \Gamma_{11} & 0 \\ \Gamma_{21} & \Gamma_{22} \end{bmatrix}, \tag{C.5}$$

where the four elements of $\Gamma(1)$ represent the cumulative impact of the TFP and demand shocks on the level of ALP and hours worked.

C.2. *Alternative Assumption in Stationarity of Hours Worked*

There is a lack of consensus about the data generating process of hours worked. Common unit root tests fail to reject the existence of a unit root in U.S. hours worked data. However, hours worked has an upper bound by construction and should not possess a permanent trend. This suggests expressing hours worked in log levels as shown in the main text. This appendix outlines the model selection exercise when hours worked is assumed to be non-stationary.

Non-stationary hours worked implies

$$LR5: \qquad d_{22,t} = d_{24,t} = 0, \tag{C.6}$$

while assuming stationary hours worked leaves $d_{22,t}$ and $d_{24,t}$ unrestricted. Table C.3 displays the additional models estimated when hours worked is assumed to be non-stationary.

Table C.4 shows the log marginal likelihood and Bayes factor for the additional SVARs when LR5 is in effect. The result indicates the importance of TVP and SV, because the TVP-SV-SVAR estimates are favored by marginal likelihood regardless of the four identification schemes. Among the additional models, however, Model 1 from the main text is still strongly favored by data, with the next smallest Bayes factor of 720 of Model 17. Therefore, assuming non-stationary hours worked does not alter my results, qualitatively.

Table C.3: List of Model Comparison, Hours Worked in Growth Rates

Model	**Identification**	**Time-Variation**
Model 17	SR1, SR2, LR1, LR2, LR4	TVP-SV-SVAR
Model 18	SR1, SR2, SR3, LR1, LR2, LR4	TVP-SV-SVAR
Model 19	SR1, SR2, LR1, LR2, LR3, LR4	TVP-SV-SVAR
Model 20	SR1, SR2, SR3, LR1, LR2, LR3, LR4	TVP-SV-SVAR
Model 21	SR1, SR2, LR1, LR2, LR4	TVP-SVAR
Model 22	SR1, SR2, SR3, LR1, LR2, LR4	TVP-SVAR
Model 23	SR1, SR2, LR1, LR2, LR3, LR4	TVP-SVAR
Model 24	SR1, SR2, SR3, LR1, LR2, LR3, LR4	TVP-SVAR
Model 25	SR1, SR2, LR1, LR2, LR4	SV-SVAR
Model 26	SR1, SR2, SR3, LR1, LR2, LR4	SV-SVAR
Model 27	SR1, SR2, LR1, LR2, LR3, LR4	SV-SVAR
Model 28	SR1, SR2, SR3, LR1, LR2, LR3, LR4	SV-SVAR
Model 29	SR1, SR2, LR1, LR2, LR4	Fixed-Parameter SVAR
Model 30	SR1, SR2, SR3, LR1, LR2, LR4	Fixed-Parameter SVAR
Model 31	SR1, SR2, LR1, LR2, LR3, LR4	Fixed-Parameter SVAR
Model 32	SR1, SR2, SR3, LR1, LR2, LR3, LR4	Fixed-Parameter SVAR

Table C.4: Log Marginal Likelihood and Bayes Factor of Additional Models

TVP-SV-SVAR	TVP-SVAR	SV-SVAR	Fixed-Parameter SVAR
[Model 17]	[Model 21]	[Model 25]	[Model 29]
-278.31	-351.19	-337.17	-907.86
(720)	($3.22e^{34}$)	($2.63e^{28}$)	($>1e^{50}$)
[Model 18]	[Model 22]	[Model 26]	[Model 30]
-299.85	-279.17	-370.19	-907.04
($1.63e^{12}$)	($1.70e^{3}$)	($5.76e^{42}$)	($>1e^{50}$)
[Model 19]	[Model 23]	[Model 27]	[Model 31]
-289.91	-298.67	-375.52	-906.79
($7.86e^{7}$)	($5.01e^{11}$)	($1.18e^{45}$)	($>1e^{50}$)
[Model 20]	[Model 24]	[Model 28]	[Model 32]
-287.61	-315.52	-327.88	-907.89
($7.88e^{6}$)	($1.04e^{19}$)	($2.43e^{24}$)	($>1e^{50}$)

Notes: Log likelihoods are reported and calculated following Geweke (1999). Bayes factors are calculated with respect to Model 1 from the main text and are reported in parentheses.

Appendix D. Non-fundamentalness

An econometric concern about the identification of news shocks is non-fundamentalness. The SVAR suffers from non-fundamentalness when the information set used by the econometrician is not sufficient to cover that of the economic agents. In other words, economic agents may form decisions using more variables than what is included in the SVAR. Therefore, the SVAR cannot reliably recover the structural shocks and impulse response functions.

D.1. Fundamentalness Tests

In this section, I show the identification of the news shock in this paper do not suffer nonfundamentalness by presenting (*i*) results from the test of sufficient information à la Forni et al. (2014), (*ii*) results from the test of fundamentalness à la Forni and Gambetti (2014), and (*iii*) a comparison of the IRFs of ALP and hours worked with respect to the news shock to the news literature.

Forni et al. (2014) and Forni and Gambetti (2014) propose tests for non-fundamentalness that base on a Factor Augmented VAR. The intuition is to use a large set of factors to capture (mostly) all relevant information by economic agents. If the structural shock of interest is orthogonal to the large factor set (and its lags), then the SVAR is fundamental because all relevant information about the shock is included. The two tests follow a similar general procedure but differ in orthogonality test which I outline below.

1. Collect a large data set of all relevant macroeconomic variables. Forni et al. (2014) adopt 107 U.S. quarterly series while Forni and Gambetti (2014) use 61.
2. Compute P principal components of the data set. Both recommend setting P=10.
3. Perform test of orthogonality. Forni et al. (2014) propose an F-test on lags of the principal components. Forni and Gambetti (2014) suggest a Granger causality test between the identified structural shocks and the principal components.

4. The SVAR is fundamental if one fails to reject the null of orthogonality.

Table D.5 reports p-values from the Forni et al. (2014) fundamentalness test on the main text SVAR. I compute the test statistics for up to 10 principal components and up to 3 lags. Recall the identification of the news shock is (*i*) news shock does not affect TFP on impact and (*ii*) news shock permanently affects TFP. The null of the Forni et al. (2014) test is that the SVAR is fundamental, i.e. the identified structural shock is orthogonal with respect to the principal components. The entries of Table D.5 suggest fundamentalness of the main text SVAR.

Table D.5: Results of the Forni et al. (2014) Fundamentalness Test

	Principal Components (from 1 to 10)									
	1	2	3	4	5	6	7	8	9	10
Lag = 1	0.2163	0.4660	0.0688	0.1140	0.1846	0.2757	0.3771	0.4794	0.5235	0.5867
Lag = 2	0.3894	0.6369	0.1805	0.2421	0.3709	0.3409	0.4833	0.3975	0.3817	0.5011
Lag = 3	0.0636	0.1260	0.0921	0.1307	0.1931	0.1962	0.2832	0.2673	0.2216	0.2219

Notes: Following Forni et al. (2014), each entry represents the p-value of the F-test on orthogonality of the news shock with respect to the first 1 to 10 principal components. The null is the SVAR is fundamental.

Table D.6 shows the Granger causality test results following Forni and Gambetti (2014). When the number of principal components are larger than 4, the test consistently supports fundamentalness in the main text SVAR.

Table D.6: Results of the Forni and Gambetti (2014) Sufficient Information Test

	P=2	P=4	P=6	P=8	P=10
Lag = 1	0.0012	0.2131	0.3525	0.4269	0.9446
Lag = 2	0.0400	0.0338	0.5211	0.1273	0.1866
Lag = 3	0.3367	0.1005	0.0444	0.0991	0.1401

Notes: Following Forni and Gambetti (2014), each entry represents the p-value of the Granger causality test (global sufficiency). The null is the SVAR is fundamental.

D.2. Robustness Check: Impulse Response Functions

Figure D.2 plots the 3-dimensional IRFs of ALP to a news shock from 1963Q1 to 2017Q4. Following identifying restriction SR2, ALP does not respond to the news shock

Fig. D.2. IRFs of ALP to a News Shock, 1963Q1 - 2017Q4

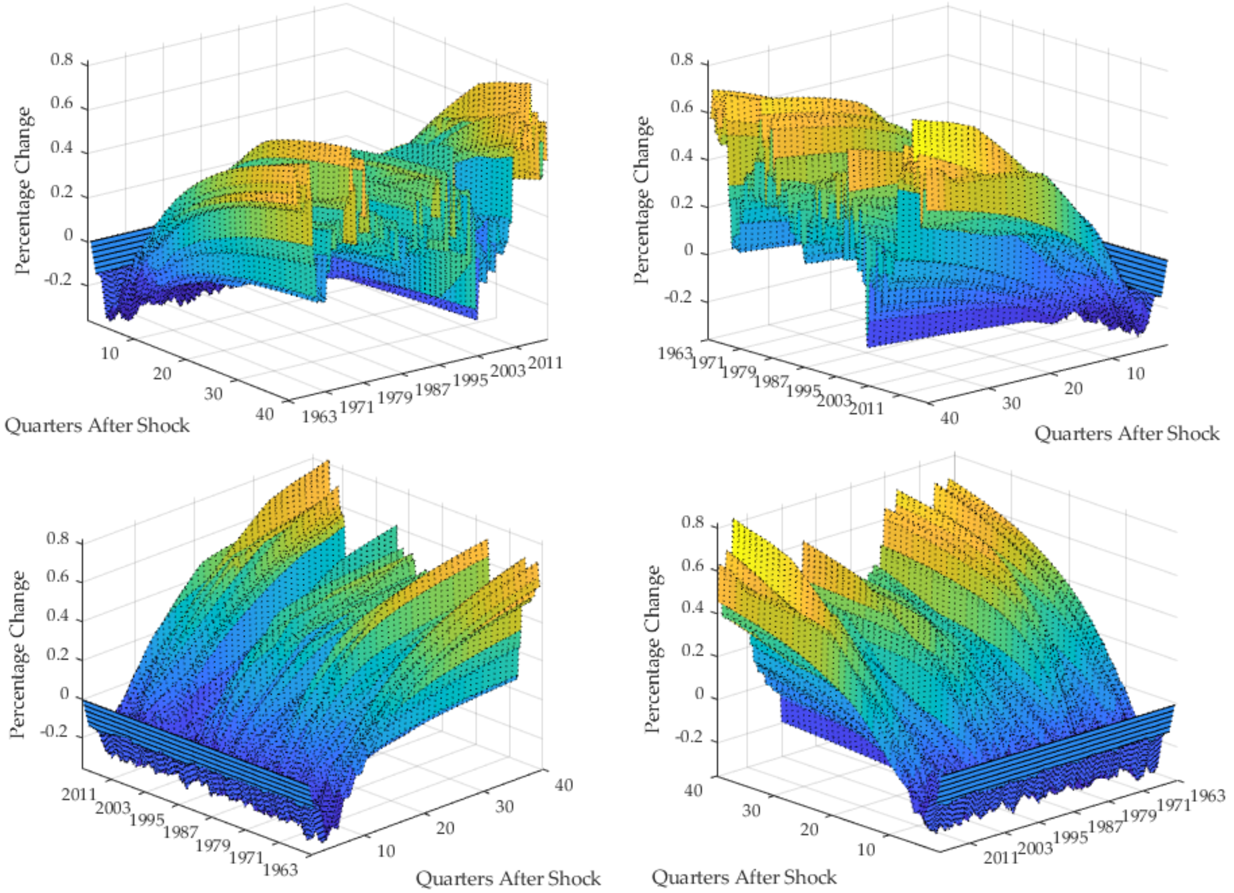

Notes: The 3-D plots show the median responses of average labor productivity to a news shock across the entire sample. The sample period is 1963Q1 to 2017Q4. X-axis: quarters after shock; y-axis: magnitude of response (percentage change); z-axis: sample date. SVAR estimated with Model 1. Plots are rotated for viewability.

on impact. The responses are negative in the short-run before turning positive eight quarters after impact. The long-run responses are positive and settle at a permanently higher state. This evidence of inverse hump-shaped responses qualitatively and quantitatively matches the consensus of a news driven expansion, e.g., Beaudry and Portier (2014), Forni et al. (2019), and Beaudry et al. (2019), among others.

Appendix E. Necessary and Sufficient Conditions of Identification Schemes

SVARs in the main text are identified with short- and long-run restrictions. Table E.7 below revisits the data favored identification scheme of Model 1. I perform the Rubio-Ramirez et al. (2010) (RRWZ henceforth) check for global identification on Model 1.

Table E.7: Identifying Restrictions of Model 1

$$\begin{bmatrix} IR_0 \\ IR_\infty \end{bmatrix} = \begin{matrix} \Delta log(x) \\ log(n) \\ \Delta log(I) \\ \Delta log(c) \\ \Delta log(s) \\ \Delta log(x) \\ log(n) \\ \Delta log(I) \\ \Delta log(c) \\ \Delta log(s) \end{matrix} \begin{bmatrix} - & 0 & 0 & 0 & 0 \\ - & - & - & - & - \\ 0 & 0 & - & 0 & 0 \\ - & - & - & - & - \\ - & - & - & - & - \\ - & 0 & - & 0 & - \\ - & - & - & - & - \\ - & 0 & - & 0 & - \\ - & 0 & - & 0 & - \\ - & - & - & - & - \end{bmatrix}$$

Notes: "-" denotes unrestricted entries; "0" denotes zero restricted entries. The columns, from left to right, denote TFP shock, labor demand shock, immigration supply shock, transitory consumption shock, and news shock.

From Table E.7, the number of identified shocks is $n = 5$, the number of column restrictions $q_1 = 1$, $q_2 = 5$, $q_3 = 1$, $q_4 = 5$, and $q_5 = 2$. The total number of column restrictions ($\sum_{j=1}^{4} q_j = 14$) is greater than $n(n-1)/2 = 10$. Following Rothenberg (1971) and Theorem 7 of Rubio-Ramirez et al. (2010), this set of restrictions is over-identified. Therefore, Model 1 and all other proposed identification schemes satisfy the necessary rank condition.

As an example, I verify RRWZ's global and local identification conditions for the selected identification scheme of Model 1. The intuition is to check for the rank condition of the restriction matrix, denoted K_0, to confirm that observational equivalence does not exist. It must satisfy necessary and sufficient conditions outlined below.

Proof. First, import K_0':

$$K_0' = \begin{bmatrix} 1 & 0 & 0 & 0 & 0 \\ 1 & 1 & 1 & 1 & 1 \\ 0 & 0 & 1 & 0 & 0 \\ 1 & 1 & 1 & 1 & 1 \\ 1 & 1 & 1 & 1 & 1 \\ 1 & 0 & 1 & 0 & 1 \\ 1 & 1 & 1 & 1 & 1 \\ 1 & 0 & 1 & 0 & 1 \\ 1 & 0 & 1 & 0 & 1 \\ 1 & 1 & 1 & 1 & 1 \end{bmatrix} \tag{E.1}$$

Then, calculate $Q_i = R_i K_0' i_j$ matrix for $i = 1 \ldots 4$. The detailed calculation step of Q_1 is shown as example. Notice that:

$$\begin{bmatrix} 0 & 0 & 0 & 0 & 0 & 0 & 0 & 0 & 0 & 0 \\ 0 & 0 & 0 & 0 & 0 & 0 & 0 & 0 & 0 & 0 \\ 0 & 0 & 1 & 0 & 0 & 0 & 0 & 0 & 0 & 0 \\ 0 & 0 & 0 & 0 & 0 & 0 & 0 & 0 & 0 & 0 \\ 0 & 0 & 0 & 0 & 0 & 0 & 0 & 0 & 0 & 0 \\ 0 & 0 & 1 & 0 & 0 & 0 & 0 & 0 & 0 & 0 \\ 0 & 0 & 0 & 0 & 0 & 0 & 0 & 0 & 0 & 0 \\ 0 & 0 & 0 & 0 & 0 & 0 & 0 & 0 & 0 & 0 \\ 0 & 0 & 0 & 0 & 0 & 0 & 0 & 0 & 0 & 0 \\ 0 & 0 & 0 & 0 & 0 & 0 & 0 & 0 & 0 & 0 \end{bmatrix} \begin{bmatrix} 1 & 0 & 0 & 0 & 0 \\ 1 & 1 & 1 & 1 & 1 \\ 0 & 0 & 1 & 0 & 0 \\ 1 & 1 & 1 & 1 & 1 \\ 1 & 1 & 1 & 1 & 1 \\ 1 & 0 & 1 & 0 & 1 \\ 1 & 1 & 1 & 1 & 1 \\ 1 & 0 & 1 & 0 & 1 \\ 1 & 0 & 1 & 0 & 1 \\ 1 & 1 & 1 & 1 & 1 \end{bmatrix}' \begin{bmatrix} 1 \\ 0 \\ 0 \\ 0 \\ 0 \end{bmatrix} = \begin{bmatrix} 0 \\ 0 \\ 0 \\ 0 \\ 0 \\ 0 \\ 0 \\ 0 \\ 0 \\ 0 \end{bmatrix}$$

Stack $R_i K_0^{'}$ on top of $\begin{bmatrix} 1 & 0 & 0 & 0 & 0 \end{bmatrix}$ to yield M_1:

$$M_1 = \left[\begin{array}{ccccc} 0 & 0 & 0 & 0 & 0 \\ 0 & 0 & 0 & 0 & 0 \\ 0 & 0 & 1 & 0 & 0 \\ 0 & 0 & 0 & 0 & 0 \\ 0 & 0 & 0 & 0 & 0 \\ 0 & 0 & 1 & 0 & 0 \\ 0 & 0 & 0 & 0 & 0 \\ 0 & 0 & 0 & 0 & 0 \\ 0 & 0 & 0 & 0 & 0 \\ 0 & 0 & 0 & 0 & 0 \\ \hline 1 & 0 & 0 & 0 & 0 \end{array}\right].$$

Following a similar procedure, calculate $M_2 ... M_5$:

$$M_2 = \begin{bmatrix} \begin{array}{ccccc} 1 & 0 & 0 & 0 & 0 \\ 1 & 0 & 0 & 0 & 0 \\ 0 & 0 & 0 & 0 & 0 \\ 0 & 0 & 0 & 0 & 0 \\ 0 & 0 & 1 & 0 & 1 \\ 1 & 0 & 1 & 0 & 0 \\ 0 & 0 & 0 & 0 & 0 \\ 0 & 0 & 0 & 0 & 0 \\ 1 & 0 & 1 & 0 & 1 \\ 0 & 0 & 0 & 0 & 0 \\ \hline 1 & 0 & 0 & 0 & 0 \\ 0 & 1 & 0 & 0 & 0 \end{array} \end{bmatrix}, M_3 = \begin{bmatrix} \begin{array}{ccccc} 1 & 0 & 0 & 0 & 0 \\ 1 & 0 & 0 & 0 & 0 \\ 0 & 0 & 0 & 0 & 0 \\ 0 & 0 & 0 & 0 & 0 \\ 0 & 0 & 0 & 0 & 0 \\ 0 & 0 & 0 & 0 & 0 \\ 0 & 0 & 1 & 0 & 0 \\ 1 & 0 & 1 & 0 & 1 \\ 1 & 0 & 1 & 0 & 1 \\ 0 & 0 & 0 & 0 & 0 \\ \hline 1 & 0 & 0 & 0 & 0 \\ 0 & 1 & 0 & 0 & 0 \\ 0 & 0 & 1 & 0 & 0 \end{array} \end{bmatrix}, M_4 = \begin{bmatrix} \begin{array}{ccccc} 0 & 0 & 0 & 0 & 0 \\ 1 & 0 & 0 & 0 & 0 \\ 0 & 0 & 0 & 0 & 0 \\ 0 & 0 & 0 & 0 & 0 \\ 0 & 0 & 0 & 0 & 0 \\ 0 & 0 & 0 & 0 & 0 \\ 0 & 0 & 1 & 0 & 0 \\ 1 & 0 & 1 & 0 & 1 \\ 0 & 0 & 0 & 0 & 0 \\ 0 & 0 & 0 & 0 & 0 \\ \hline 1 & 0 & 0 & 0 & 0 \\ 0 & 1 & 0 & 0 & 0 \\ 0 & 0 & 1 & 0 & 0 \\ 0 & 0 & 0 & 1 & 0 \end{array} \end{bmatrix},$$

and

$$M_5 = \begin{bmatrix} 1 & 0 & 0 & 0 & 0 \\ 0 & 0 & 1 & 0 & 0 \\ 0 & 0 & 0 & 0 & 0 \\ 0 & 0 & 0 & 0 & 0 \\ 0 & 0 & 0 & 0 & 0 \\ 0 & 0 & 0 & 0 & 0 \\ 0 & 0 & 0 & 0 & 0 \\ 0 & 0 & 0 & 0 & 0 \\ 0 & 0 & 0 & 0 & 0 \\ 0 & 0 & 0 & 0 & 0 \\ \hline 1 & 0 & 0 & 0 & 0 \\ 0 & 1 & 0 & 0 & 0 \\ 0 & 0 & 1 & 0 & 0 \\ 0 & 0 & 0 & 1 & 0 \\ 0 & 0 & 0 & 0 & 1 \end{bmatrix}$$

It is straightforward to verify that the ranks of matrices M_1 to M_5 are $[2, 4, 4, 5, 5]$. Therefore, K_0 is locally identified. $\square$

Appendix F. Priors and Bayesian Sampling

F.1. Priors and Pre-estimation

Table F.8 shows the conjugate priors for three sets of initializations. Let $\bar{x}$ denote the OLS/ML estimate of parameter x. I use the first $\tau = 40$ observations (1953Q1 - 1962Q4) as a training sample to estimate prior values $\overline{B}, \overline{VB}, \overline{a}$, and $log(\overline{h})$ via OLS or MLE.[4] Block $\mathbb{B}$'s posterior distribution is truncated to ensure stationary draws. I also choose priors for the covariance matrices of the innovations that govern the law of motions for the aforementioned TVP-SV-VAR parameters. They control the size of the search steps in the MCMC samplers. Reported in Table F.8, the calibration of the tightness and re-scaling constants is set to allow for proper acceptance rate for convergence, while accommodating necessary time-variation.

Table F.8: Priors

$\mathbb{B}_0 \sim N(\overline{B}, \kappa_B \cdot \overline{VB})$	$Q_i \sim IW(\kappa_Q^2 \overline{VB}, \tau)$
$a_0 \sim N(\overline{a}, \kappa_a \cdot I_3)$	$S_i \sim IW(\kappa_s^2 \cdot I_3,\ 1 + dim\, a)$
$log(h_0) \sim N(log(\overline{h}), \kappa_h \cdot I_3)$	$W_i \sim IG(\kappa_W^2, 2)$

Notes: N denotes normal; IW denotes Inverted-Wishart; IG denotes Inverse Gamma. $\kappa_B = 4$, $\kappa_a = 4$, and $\kappa_h = 10$ are tightness constants. $\kappa_Q^2 = 0.24$, $\kappa_s^2 = 5 \times 10^{-3}$, and $\kappa_W^2 = 1 \times 10^{-3}$ are re-scaling factors.

F.2. Sampling Algorithm

I provide details of the Metropolis-within-Gibbs sampler, which closely follow Canova and Perez-Forero (2015).

Draw Reduced-form Coefficients, $\mathbb{B}$ The drawing of the reduced-from coefficients $\mathbb{B}$ relies on the Carter-Kohn algorithm. Carter and Kohn (1994) show that the combination of the Kalman filter and a backward recursion algorithm gives an efficient way of solving for the states of a state-space model.

[4] I adopt Christopher Sims' **csminwel** package with a search tolerance of 1×10^{-4} in obtaining the ML estimator.

Particularly, the Carter-Kohn algorithm contains the following steps:

1 The Kalman filter provides an estimate of the mean $\mathbb{B}_{T|T}$ and variance $P_{T|T}$.

2 Given the Kalman estimates, take a random draw of a multivariate normal with mean $\mathbb{B}_{T|T}$ and covariance $P_{T|T}$.

3 At $T-1$, use Kalman update equations to recursively obtain $\mathbb{B}_{T-1|T-1,\mathbb{B}_T}$ and $P_{T-1|T-1,\mathbb{B}_T}$. Draw $\mathbb{B}_{T-1}$ from $N(\mathbb{B}_{T-1|T-1,\mathbb{B}_T}, P_{T-1|T-1,\mathbb{B}_T})$.

4 Repeat step 2 for $t = T-2, T-3, ..., 1$.

Therefore, the Carter-Kohn algorithm yields a series of draws of $\mathbb{B}$ for $t = 1, \cdots, T$.

Draw Structural Coefficients, $\tilde{\mathbb{B}}$ Given the current draw of the reduced-form coefficient $\mathbb{B}_i$, the last draw of the contemporaneous matrix $A_{0,i-1}$, and the last draw of the standard deviations of the structural shocks Σ_{i-1}, I impose long-run restrictions. As discussed, long-run restrictions create non-linearity in the VAR parameter space. Therefore, long-run restrictions need to be imposed in the sampler during each draw.

Compute the long-run cumulative impact matrix

$$D_i^T = J(I_2 - \mathbb{B}_i^T)^{-1} J' A_{0,i-1}^T \Sigma_{i-1}^T, \tag{F.1}$$

where $J = [I_2 \ldots 0_2]$ is a selection matrix. Denote d_{jk} the elements in D_i^T. Setting the respective d_{jk} to zero achieves the long-run restriction.

Let the restricted long-run cumulative matrix be $\mathbb{D}_i$, solve for the draws restricted structural coefficient matrix B_i by reversing equation F.1. Lastly, evaluate the eigenvalues of $\tilde{\mathbb{B}}$ and discard the draws that have eigenvalues outside the unit circle.

Draw Impact Coefficients, A_0 Given $\tilde{\mathbb{B}}_t$, the state-space model can be re-written as

$$A_{0,t}(z_t - X_t' \tilde{\mathbb{B}}_t) \equiv A_{0,t} \hat{z}_t = \Sigma_t \epsilon_t.$$

Let $vec(A_t) = S_A f(a_t) + s_A$, where S_A and s_A are selection matrices of ones and zeros. Reparametrize the model as

$$(\hat{z}_t{}' \otimes I)(S_A f(a_t) + s_A) = \Sigma_t \epsilon_t.$$

Therefore the system of regression only contains linear restrictions, with observation equation

$$(\hat{z}_t{}' \otimes I) s_A = -(\hat{z}_t{}' \otimes I) S_A f(a_t) + \Sigma_t \epsilon_t.$$

and state equation

$$f(a_t) = f(a_{t-1}) + \eta_t.$$

Given initial $f(a_t)_{0|0}$ and $P_{0|0}$, the Extended Kalman Filter (EKF) gives updates of $f(a_t)$ and its covariance matrix. The smoothed estimates are denoted $f(a_t)^*_{T|T}$ and $P^*_{T|T}$.

The algorithm of drawing $f(a)$ is:

1 Given (z^T, V^{i-1}), compute $f(a_t)^{*i-1}_{T|T}$ and $P^{*i-1}_{T|T}$.

2 For $t = 1, ..., T$, draw a candidate $f(a_t^+)$ from $p_*[f(a_t)|f(a_t^{i-1})]$.

3 Compute $\theta = \frac{|(f(a^+)^T) \times p_*[f(a_t)|f(a_t^{i-1})]^T}{|(f(a)^T) \times p_*[f(a^T)|f(a_t^{i-1})]}$.

4 Draw $\mu \sim U(0,1)$. Accept new draw as $f(a^i)^T = f(a^+)^T$ if $\mu < \theta$; otherwise keep old draw.

5 Given $(z^T, f(a^i)^T)$, draw $V^i \sim IW(v, \bar{V}^{-1})$, where $\bar{V}^{-1}$ is the sum of squared errors in the state equation of $f(a)$.

Draw Stochastic Volatility, Σ Conditional on the current draws $(\tilde{\mathbb{B}}_i^T, a_i^T)$, the left hand side of the model equation $A(a_t) y_t = \Sigma_t \epsilon_t$ is known. Taking square and log each element of this vector yields a linear state-space system

$$z_t^* = 2log(\sigma_t) + 2log(\epsilon_t);$$

$$log(\sigma_t) = log(\sigma_{t-1}) + \eta_t,$$

where $z_t^* \equiv log(z_t)^2$. However, this system is not Gaussian, because each element of 2log(ϵ_t) is distributed log χ^2. These shocks are approximated with a 10-component mixture of normals. Following Omori et al. (2007), auxiliary variables s_i^T are introduced and drawn conditional on $(\tilde{\mathbb{B}}_i^T, a_i^T, \sigma_{i-1}^T)$ to keep track of the normal mixtures. The state-space system is Gaussian given the approximation $(\tilde{\mathbb{B}}_i^T, a_i^T, \sigma_i^T)$. The draws of σ_i^T are generated and evaluated with the Carter-Kohn algorithm.

Draw Hyperparameter Block, $\mathcal{V}$ Draw the hyperparameters $\mathcal{V}_i$ given $(\tilde{\mathbb{B}}_i^T, A_{0,i}^T, \Sigma_i^T, z_i^T)$ according to the specified distributions shown in Table F.8.

Appendix G. Convergence Diagnosis

I adopt two methods to examine convergence of the sampling routine to the ergodic distribution. First, I plot the sequence of retained draws in Figure G.3 for the Model 1 SVAR estimated with TVP and SV. If the sampler has converged, variation for each coefficient estimates between the retained draws should be small and does not show pattern of memory. All three panels exhibit minimal and trendless fluctuations for recursive means calculated with every 20 draws. This evidence supports successful convergence of the Bayesian sampler.

Next, I evaluate the numerical accuracy of the sampler. Following Geweke (2005), I compute Inefficiency Factor (IF) for each block of estimated coefficients. IF is a measurement of serial correlation between MCMC draws. Following Primiceri (2005), the common satisfactory range of IF values of parameters estimated with a TVP-SV-SVAR is between 4 to 75. Table G.9 displays the descriptive statistics of IF values for each sampling block. The majority of the IFs is below 75. The impact coefficients $(A_{0,t})$ average slightly higher at around 81, which is common in the TVP-SV-SVAR literature. Therefore, the IFs suggest satisfactory convergence of the sampler.

Table G.9: Inefficiency Factors

	Median	Mean	Min	Max	10^{th} Pct	90^{th} Pct
$\mathbb{B}_i$	54.49	58.48	24.81	92.21	43.04	76.11
$A_{0,i}$	81.36	82.44	0.696	43.48	70.86	90.51
Σ_i	4.52	24.51	0.59	70.97	1.75	64.55

Fig. G.3. Sequence of Retained Draws

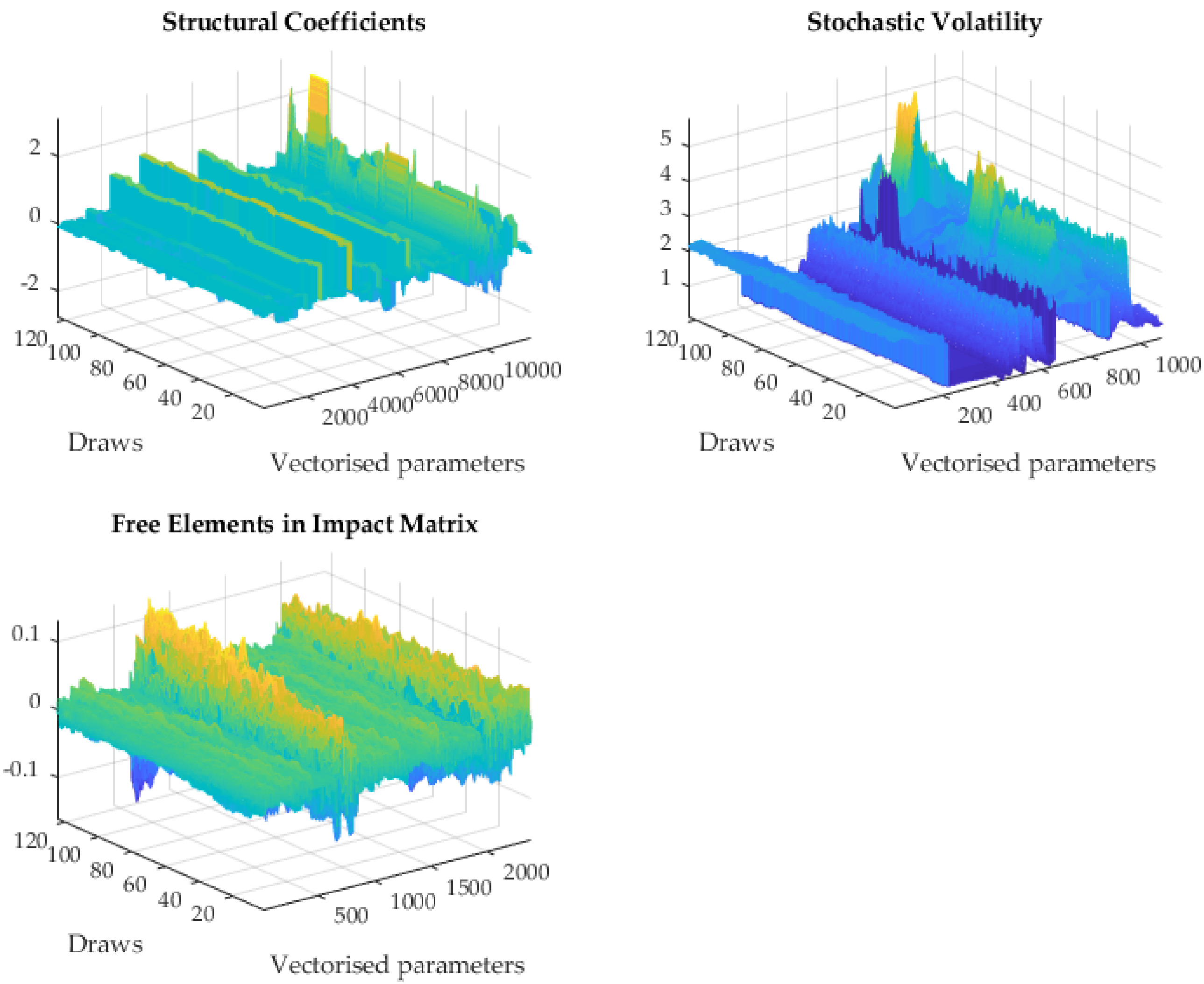

Notes: The 3-D plots show sequence of retained draws for all estimated parameters in the benchmark SVAR (Model 1). X-axis: number of draws; y-axis: magnitude of estimated parameters; z-axis: number of estimated vectorised parameters.

Appendix H. Log Marginal Likelihood

This section outlines the details in computing the log marginal likelihood of a SVAR post estimation. I adopt the harmonic mean estimator following Geweke (1999).

First, let

$$p(z|M_k) = \int p(z|\theta_k, M_k)p(\theta_k|M_k)d\theta_k \tag{H.1}$$

be the marginal likelihood of model k. For the class of TVP-SV-SVARs outlined in this paper, an analytical expression of the marginal likelihood is unavailable due to the degree of parameterization and non-linearity. The Gibbs sampler provides a convenient approximation. Following Geweke (1999), I compute the marginal likelihoods of the competing models using the harmonic mean method. Given any distribution $g(\theta)$, the inverse of the marginal likelihood $p(z)^{-1}$ can be written as the expected value of the product of the likelihood $p(z|\theta)$ and the prior $p(\theta)$ for the model

$$p(z)^{-1} = E[\frac{g(\theta)}{p(z|\theta)p(\theta)}|z]. \tag{H.2}$$

In practice, I estimate log marginal likelihood of equation (H.2) as follows. First, I use the Kalman filter to compute the log prior density. This is done by summing all log prior densities of the latent variables ($\mathbb{B}$, A_0, Σ) and their respective hyperparameters (Q, S, W) according to the probability distribution functions (PDFs) of the priors. $p(z|\theta)$ is evaluated by updating the measurement equation of the Kalman filter. Geweke (1999) suggests using a truncated normal distribution for $g(\theta)$. The following sections detail the computation of each elements in equation (H.2).

H.1. Estimating $p(z|\theta)$

The likelihood for a state space model $p(z|\theta)$ can be evaluated with the Kalman filter. For a state space model of the following representation,

$$z_t = X'\beta_t + (A_t)^{-1}\Sigma_t\epsilon_t,\ \ \epsilon_t \sim N(0, I), \tag{H.3}$$

and

$$\beta_t = F\beta_{t-1} + u_t,\ \ u_t \sim N(0, \mathcal{V}), \tag{H.4}$$

the linear-Gaussian Kalman filter recursion is given by

$$\beta_{t|t-1} = F\beta_{t-1|t-1} \tag{H.5}$$

$$P_{t|t-1} = FP_{t-1|t-1}F' + \mathcal{V}, \tag{H.6}$$

$$\eta_{t|t-1} = z_t - X_t\beta_{t|t-1}, \tag{H.7}$$

$$f_{t|t-1} = XP_{t|t-1}X' + \eta_t\eta_t', \tag{H.8}$$

$$K = P_{t|t-1}X'f_{t|t-1}^{-1}, \tag{H.9}$$

$$\beta_{t|t} = \beta_{t|t-1} + K\eta_{t|t-1}, \tag{H.10}$$

and

$$P_{t|t} = P_{t|t-1} - KXP_{t|t-1}. \tag{H.11}$$

The first two equations (H.5) and (H.6) are the prediction equations that provide the value and the estimated variance of the state variable one period ahead. Equation (H.7) computes the prediction error, whereas equation (H.8) computes the variance of the prediction error. The Kalman gain, usually considered as the weight attached to the prediction error, is calculated in equation (H.9). The last two equations (H.10) and (H.11) are the updating equations that give one period ahead estimates of the states.

Given estimates from the Kalman filter, the log likelihood is computed as

$$ln[p(z|\theta)] = -\frac{Tk}{2}ln(2\pi) - \frac{1}{2}\sum_{t=1}^{T}|P_t| - \frac{1}{2}\eta_t P_t^{-1}\eta_t'. \tag{H.12}$$

H.2. Estimating $p(\theta)$

The prior densities $p(\theta)$ of states and hyperparameters are computed directly from their probability density functions. Given the Gaussian states and the inverse-Wishart priors of hyperparameters, $p(\theta)$ is equal to the sum of all individual densities. In the case of TVP-SVARs with no SV and SV-SVARs with no TVP, the log density of the respective missing states is 1.

H.3. Estimating p(z)

As in equation H.2 in the main text, the marginal likelihood of a model is defined as

$$p(z)^{-1} = E[\frac{g(\theta)}{p(z|\theta)p(\theta)}|z]. \tag{H.13}$$

In practice, this is estimated as

$$\hat{p(z)}^{-1} = \frac{1}{M}\sum_{j=1}^{M}\frac{g(\theta)}{p(z|\theta)p(\theta)}, \tag{H.14}$$

where M is the number of retained draws. The distribution of $g(\theta)$ is selected as a truncated normal. Geweke (1999) discusses the selection of $g(\theta)$ in detail.

Appendix I. Additional IRFs and Robustness Check

I.1. Additional IRFs, FEVDs, and Plots of TVPs

Figure I.4 displays the IRFs of immigration with respect to a labor demand shock with error bands at 2, 4, 8, and 16 quarters post shock. The responses fluctuate around zero for all horizons with large error bands. Therefore, there is no quantitatively meaningful effect of a labor demand shock on immigration.

The IRFs of immigration with respect to a transitory consumption shock are in Figure I.5. The hump-shaped IRFs peak at two quarters after the shock and plateau after four years as shown in the upper and lower right panels. The effect of a transitory consumption shock on immigration appears time-invariant. It does not appear to co-move with either changes in immigration policy nor the business cycle. The evidence of a positive but transitory response of immigration to a transitory consumption shock at the business cycle horizons is in line with the economic theory about direct and indirect incentives of immigration. First, an increase in aggregate demand through expenditure attracts immigrants because immigrants react to economic incentives (Lucas 1975). Second, a larger aggregate demand raises output growth followed by a temporary increase in aggregate supply. Therefore, a temporary boost in average productivity due to the demand shock provides an added incentive to migrate, as discussed in Section 4.2.1.

Figures I.10 and I.11 plot the FEVDs of the immigration shock on all variables and the immigration FEVD with respect to macroeconomic shocks from 1963Q1 to 2017Q4. They are plotted on selected forecast horizons of 4, 8, 20, and 32 quarters.

Figures I.12 and I.13 illustrate the impact coefficient of hours worked with respect to the immigration supply shock ($a_{23,t}$), terms spread with respect to the immigration shock ($a_{53,t}$), consumption with respect to the immigration supply shock ($\alpha_{43,t}$), and term spread with respect to the TFP shock ($\alpha_{51,t}$). Similar to the discussion in Section 4.2 of the main text, the unrestricted estimates are small and do not exhibit obvious dependency with respect to the business cycle or the state of the immigration policy regime.

Table I.10: Additional FEVDs with respect to Immigration Supply Shock

Variable	Quarter \ Date	1980Q1	1986Q1	1990Q1	2004Q1	2010Q1
	2	0.0038	0.0038	0.0034	0.0035	0.0052
	4	0.0126	0.0070	0.0102	0.0079	0.0079
Hours Worked	20	0.0203	0.0144	0.0185	0.0201	0.0101
	$\rightarrow\infty$	0.0131	0.0110	0.0167	0.0144	0.0080

Notes: Results based on TVP-SV-SVAR estimated with Model 1. The long-run ($\rightarrow\infty$) FEVD is defined as a forecast horizon of 40 quarters. Selected immigration policy dates correspond to the Refugee Act of 1980, the IRCA of 1986, the IMMACT of 1990, the H1-B Act of 2004, and Operation Streamline of 2010.

Table I.11: Posterior Tunnels of FEVDs to Immigration Supply Shock

Variable	Qtr \ Date	1980Q1	1986Q1	1990Q1	2004Q1	2010Q1
ALP	2	0.0065-0.0192	0.0066-0.0203	0.0060-0.0187	0.0065-0.0205	0.0052-0.0182
	4	0.0088-0.0411	0.0118-0.0465	0.0146-0.0424	0.0119-0.0424	0.0148-0.0499
	20	0.0204-0.1328	0.0082-0.1445	0.0193-0.0925	0.0224-0.1006	0.0150- 0.0773
	$\rightarrow \infty$	0.0201-0.1330	0.0082-0.1444	0.0193-0.0950	0.0215-0.1007	0.0150-0.0773
HW	2	0.0015-0.0070	0.0019-0.0075	0.0012-0.0067	0.0009-0.0079	0.0023- 0.0086
	4	0.0044-0.0162	0.0028-0.0351	0.0058-0.0166	0.0044-0.0170	0.0040-0.0167
	20	0.0061-0.0568	0.0031-0.0495	0.0061-0.0416	0.0042-0.0489	0.0039-0.0311
	$\rightarrow \infty$	0.0053-0.0397	0.0025-0.0338	0.0048-0.0352	0.0063-0.0340	0.0029- 0.0214
Immigration	2	0.4381-0.5207	0.4415-0.5276	0.4484-0.5205	0.4460-0.5242	0.4296- 0.5155
	4	0.4642-0.5860	0.4578-0.6068	0.4508-0.6088	0.4709-0.5999	0.4392-0.5794
	20	0.3389-0.4482	0.3082-0.4374	0.3264-0.4866	0.2949-0.4670	0.2700-0.4570
	$\rightarrow \infty$	0.2570-0.3527	0.2383-0.3399	0.2583-0.3887	0.2503-0.3688	0.2345- 0.3604
Consumption	2	0.2621-0.3715	0.2704-0.3675	0.2678-0.3872	0.2678-0.3752	0.2742-0.3673
	4	0.0990-0.3278	0.1175-0.3028	0.1743-0.3264	0.1337-0.3831	0.1518-0.3442
	20	0.0447-0.2027	0.0543-0.2394	0.0926-0.2464	0.0614-0.2815	0.0460-0.2407
	$\rightarrow \infty$	0.0396-0.1869	0.0497-0.2160	0.0865-0.2309	0.0561-0.2661	0.0388-0.2261
Term Spread	2	0.3074- 0.3876	0.0975-0.3829	0.3021-0.3751	0.2947-0.3778	0.3179-0.4030
	4	0.2071-0.4133	0.2440-0.4517	0.2896-0.4481	0.2477-0.4422	0.3518-0.4661
	20	0.1162-0.3286	0.1505-0.3349	0.2041-0.4112	0.1460-0.3881	0.0973-0.4458
	$\rightarrow \infty$	0.1080-0.2961	0.1258-0.2937	0.1696-0.3736	0.1203-0.3694	0.0761-0.4127

Notes: Results based on TVP-SV-SVAR estimated with Model 1. The posterior tunnels are 16-84%. The long-run ($\rightarrow \infty$) FEVD is defined as a forecast horizon of 40 quarters. ALP denotes average labor productivity. HW denotes hours worked. Selected immigration policy dates correspond to the Refugee Act of 1980, the IRCA of 1986, the IMMACT of 1990, the H1-B Act of 2004, and Operation Streamline of 2010.

Table I.12: Posterior Tunnels of Immigration FEVDs to Macroeconomic Shocks

Shock	Qtr \ Date	1980Q1	1986Q1	1990Q1	2004Q1	2010Q1
TFP	2	0.1711-0.1958	0.1691-0.1939	0.1663-0.1910	0.1700-0.1955	0.1703-0.1927
	4	0.0955-0.1175	0.0954-0.1130	0.1009-0.1169	0.0978-0.1113	0.0993-0.1155
	20	0.0503-0.0826	0.0603-0.0748	0.0636-0.0774	0.0559-0.0784	0.0578- 0.0872
	$\rightarrow\infty$	0.0371-0.0681	0.0469-0.0663	0.0556-0.0665	0.0487-0.0631	0.0482-0.0700
LD	2	0.2732-0.3598	0.2729-0.3645	0.2738-0.3646	0.2718-0.3565	0.2808- 0.3713
	4	0.3034-0.4140	0.2875-0.4221	0.2752-0.4313	0.2809-0.4115	0.2971-0.4400
	20	0.3691-0.5863	0.4098-0.5151	0.3057-0.5059	0.3356-0.6012	0.3317-0.6319
	$\rightarrow\infty$	0.3957-0.6907	0.4461-0.5549	0.3595-0.5170	0.3914-0.5236	0.3968- 0.6708
TC	2	0.0034-0.0091	0.0033-0.0086	0.0028-0.0090	0.0039-0.0091	0.0035- 0.0100
	4	0.0030-0.0083	0.0027-0.0097	0.0028-0.0094	0.0042-0.0093	0.0030-0.0093
	20	0.0068-0.0146	0.0071-0.0133	0.0076-0.0157	0.0087-0.0164	0.0089-0.0124
	$\rightarrow\infty$	0.0080-0.0157	0.0087-0.0140	0.0075-0.0204	0.0103-0.0193	0.0099- 0.0156
News	2	0.0067-0.0199	0.0028-0.0148	0.0036-0.0156	0.0023-0.0145	0.0048-0.0195
	4	0.0056-0.0116	0.0035-0.0107	0.0046-0.0108	0.0046-0.0095	0.0050-0.0117
	20	0.0068-0.1359	0.0344-0.1523	0.0604-0.1767	0.0384-0.1518	0.0150-0.1165
	$\rightarrow\infty$	0.0069-0.2079	0.0473-0.2413	0.0847-0.1835	0.0992-0.2479	0.0199-0.1700

Notes: Results based on TVP-SV-SVAR estimated with Model 1. The posterior tunnels are 16-84%. The long-run ($\rightarrow\infty$) FEVD is defined as a forecast horizon of 40 quarters. TFP denotes total factor productivity. LD denotes labor demand. TC denotes transitory consumption. Selected immigration policy dates correspond to the Refugee Act of 1980, the IRCA of 1986, the IMMACT of 1990, the H1-B Act of 2004, and Operation Streamline of 2010.

Fig. I.4. IRFs of Immigration to a Labor Demand Shock at Selected Horizons

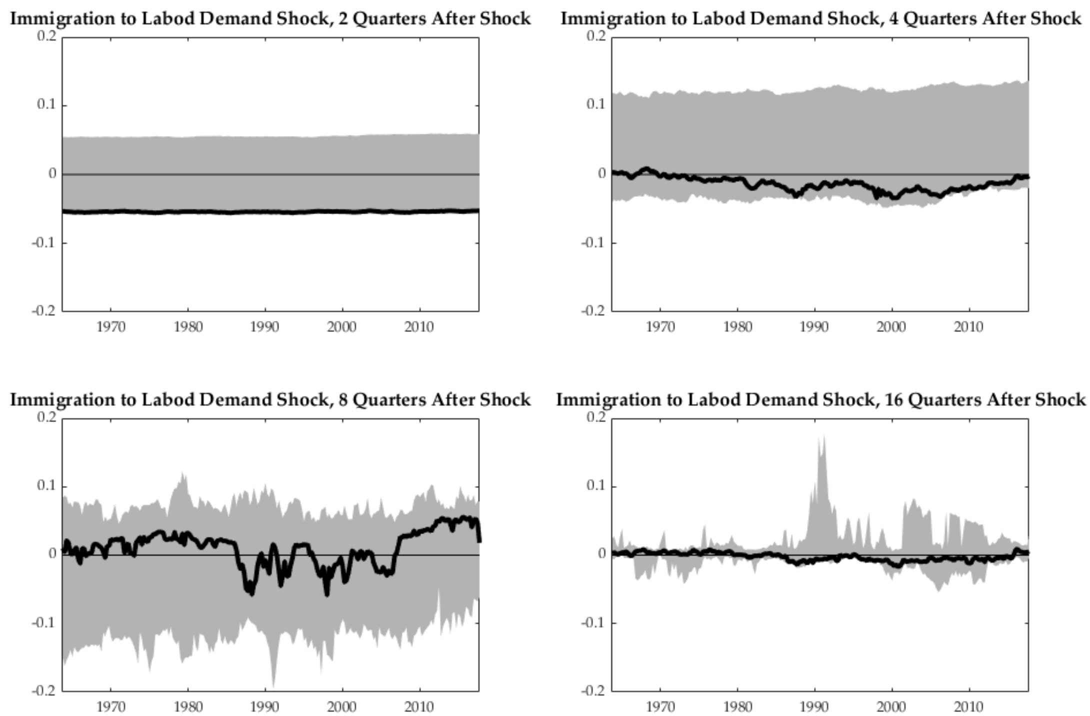

Notes: The solid (black) lines are median responses of immigration to a labor demand shock at 2, 4, 8, and 16 quarters after initial shock. Gray shaded areas are 16-84% posterior tunnels. SVAR estimated with Model 1.

Fig. I.5. IRFs of Immigration to a Transitory Consumption Shock at Selected Horizons

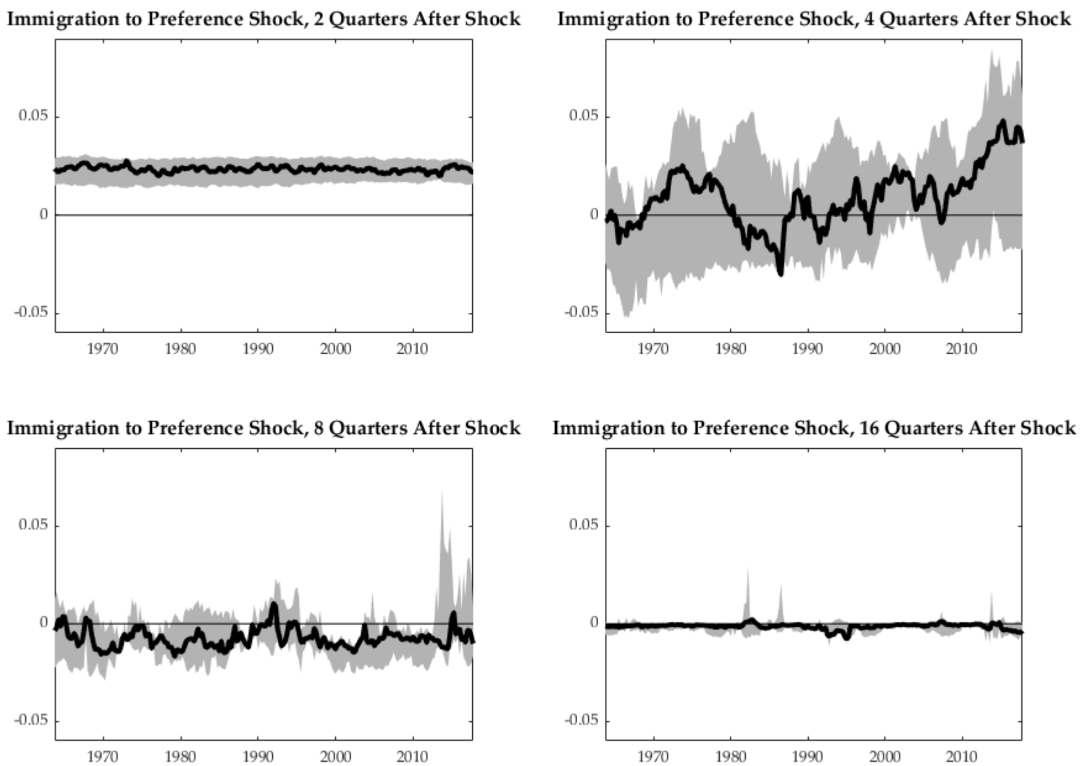

Notes: The solid (black) lines are median responses of immigration to a transitory consumption shock at 2, 4, 8, and 16 quarters after initial shock. Gray shaded areas are 16-84% posterior tunnels. SVAR estimated with Model 1.

Fig. I.6. IRFs of Hours Worked to an Immigration Supply Shock at Selected Horizons

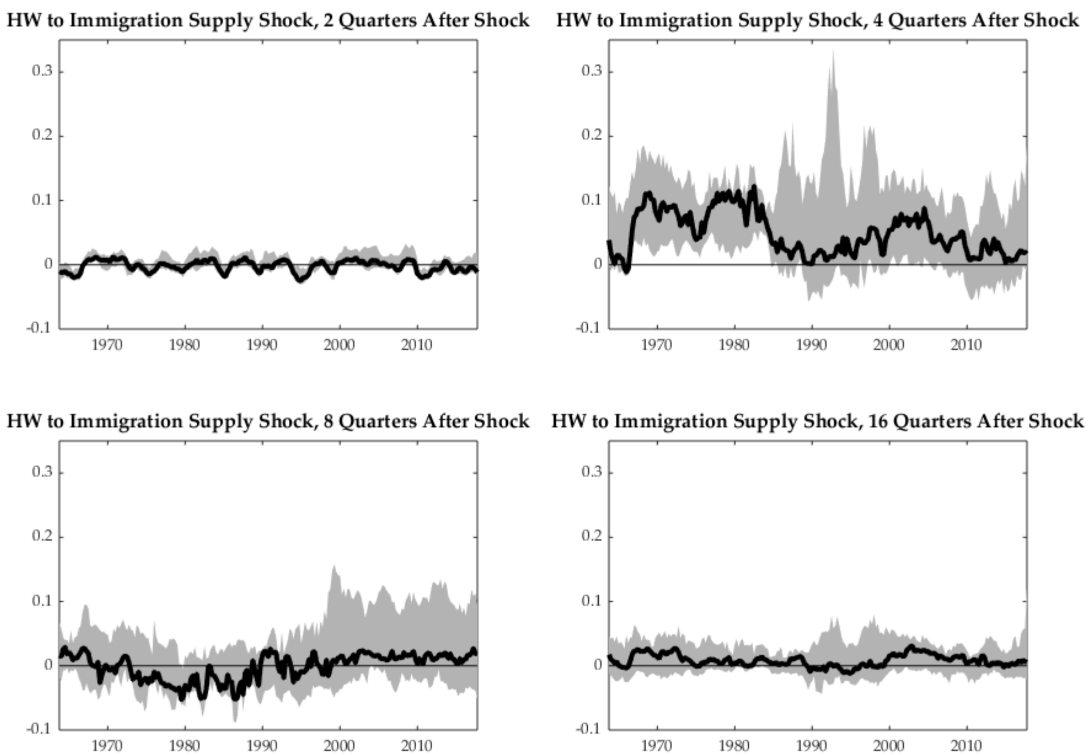

Notes: The solid (black) lines are median responses of hours worked to an immigration supply shock at 2, 4, 8, and 16 quarters after initial shock. Gray shaded areas are 16-84% posterior tunnels. SVAR estimated with Model 1.

Fig. I.7. IRFs of Consumption to an Immigration Supply Shock at Selected Horizons

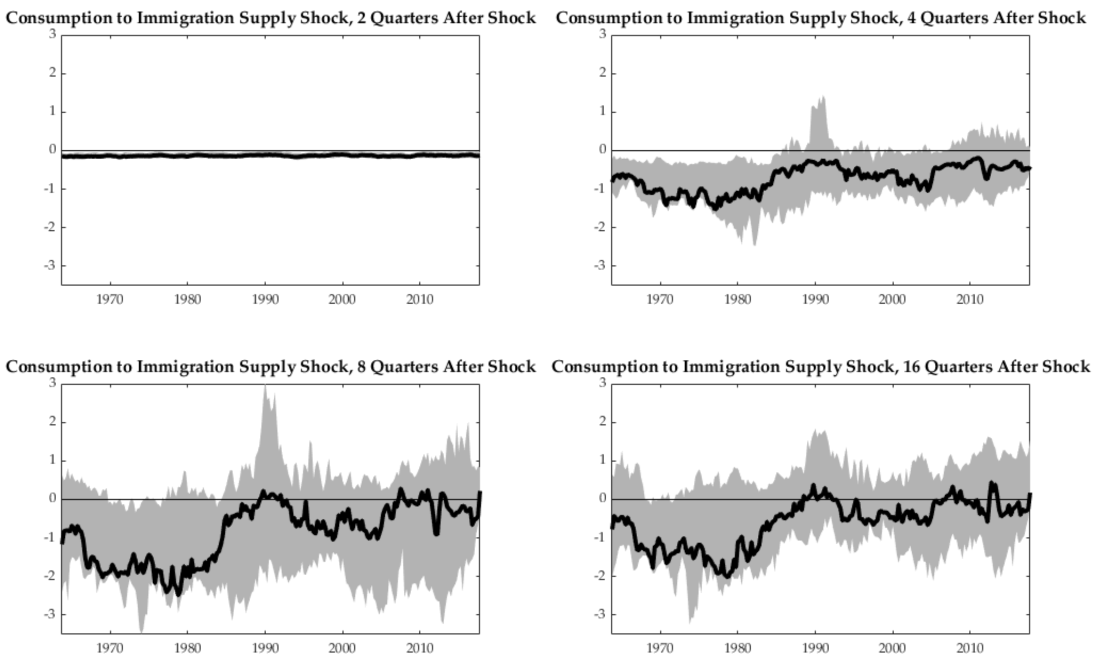

Notes: The solid (black) lines are median responses of consumption to an immigration supply shock at 2, 4, 8, and 16 quarters after initial shock. Gray shaded areas are 16-84% posterior tunnels. SVAR estimated with Model 1.

Fig. I.8. IRFs of Immigration to a TFP Shock at Selected Horizons

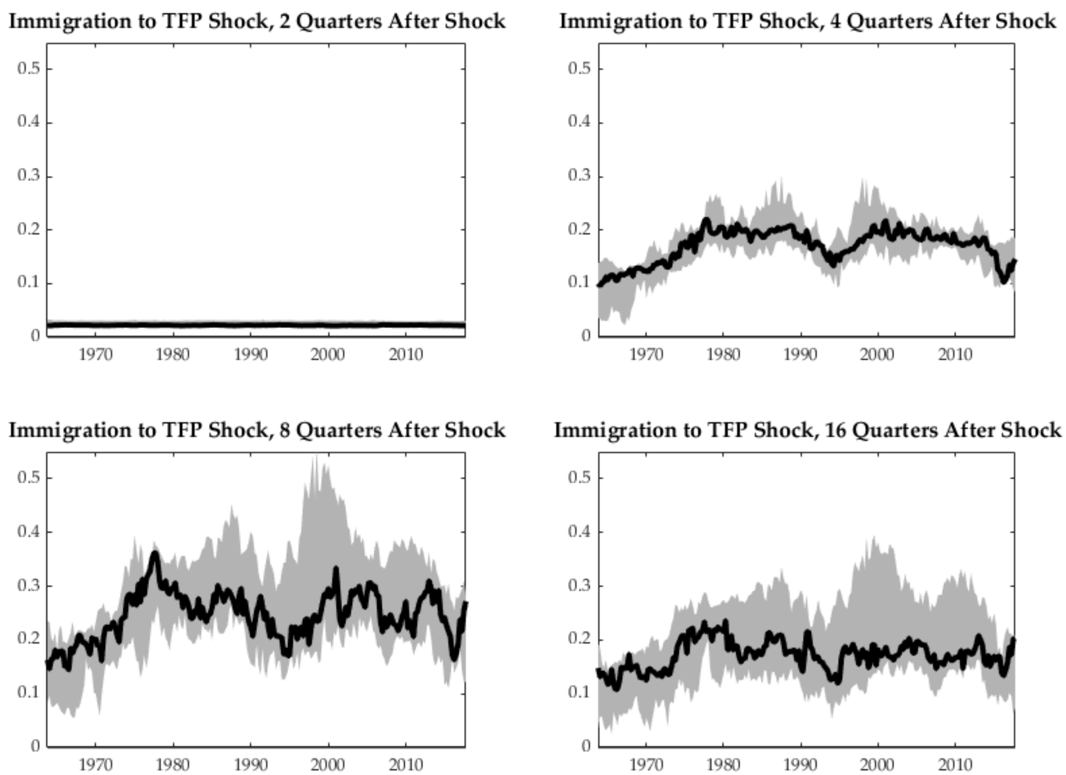

Notes: The solid (black) lines are median responses of immigration to a TFP shock at 2, 4, 8, and 16 quarters after initial shock. Gray shaded areas are 16-84% posterior tunnels. SVAR estimated with Model 1.

Fig. I.9. IRFs at Four Quarters Post Selected Immigration Policy Dates

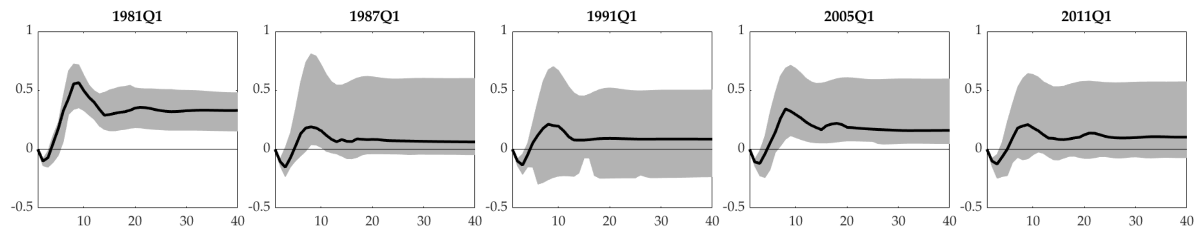

(a) ALP with respect to an immigration supply shock, estimated with Model 1

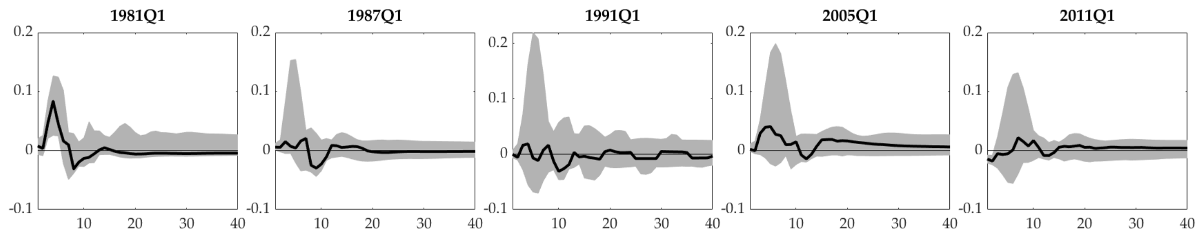

(b) Hours worked with respect to an immigration supply shock, estimated with Model 1

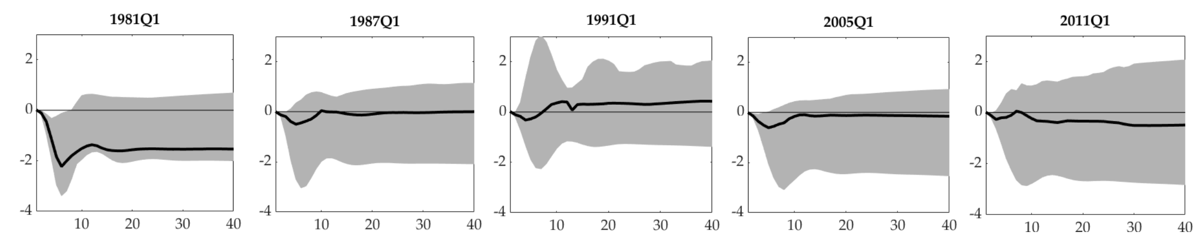

(c) Consumption with respect to an immigration supply shock, estimated with Model 1

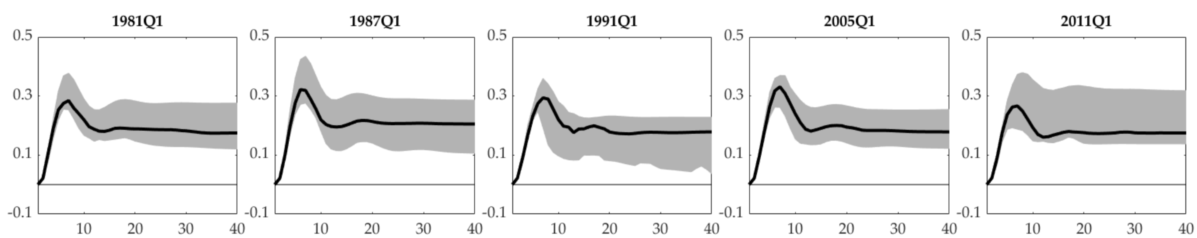

(d) Immigration with respect to a TFP shock, estimated with Model 1

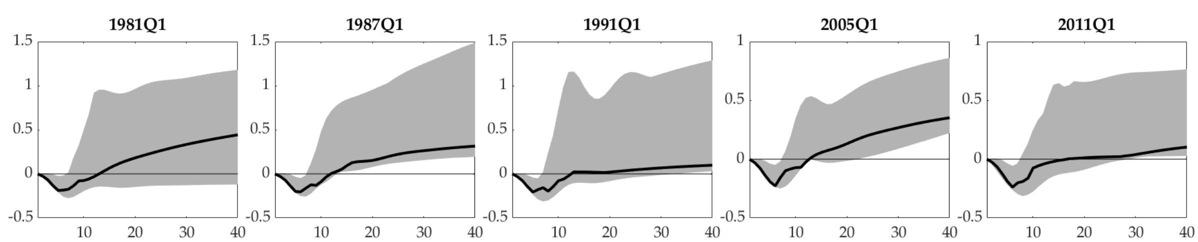

(e) Immigration with respect to a news shock, estimated with Model 1

Notes: The solid (black) lines are median responses at selected immigration policy dates. Gray shaded areas are 16-84% posterior tunnels. X-axis: sample date; y-axis: magnitude of response (percentage change in (a), (c), (d), (e), log points in (b)). Selected dates are 1981Q1, 1987Q1, 1991Q1, 2005Q1, 2011Q1.

Fig. I.10. FEVDs of Immigration Supply Shock, 1963Q1 - 2017Q4

(a) Forecast Horizon: 4 Quarters

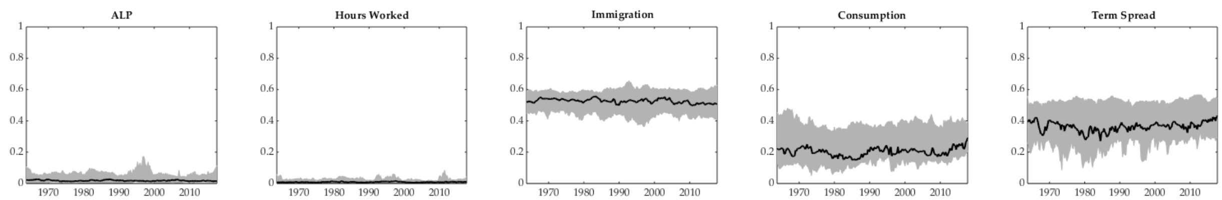

(b) Forecast Horizon: 8 Quarters

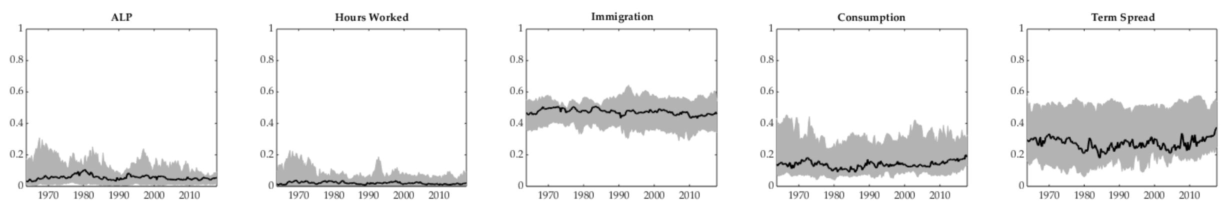

(c) Forecast Horizon: 20 Quarters

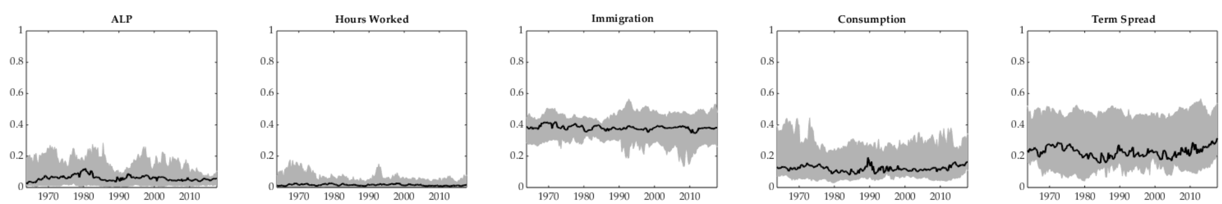

(d) Forecast Horizon: 32 Quarters

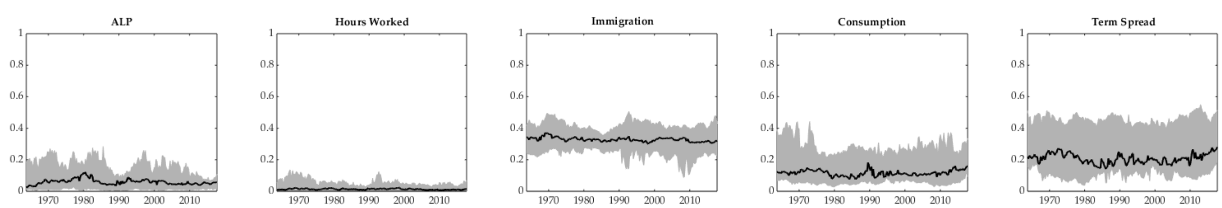

Notes: The solid (black) lines are median values of forecast error variance decompositions at 4, 8, 20, and 32 quarters after initial shock. Gray shaded areas are 16-84% posterior tunnels. SVAR estimated with Model 1.

Fig. I.11. Immigration FEVDs of Macroeconomic Shocks, 1963Q1 - 2017Q4

(a) Forecast Horizon: 4 Quarters

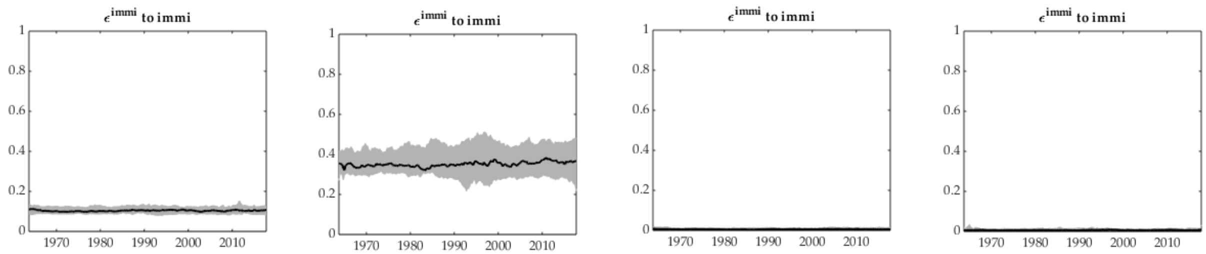

(b) Forecast Horizon: 8 Quarters

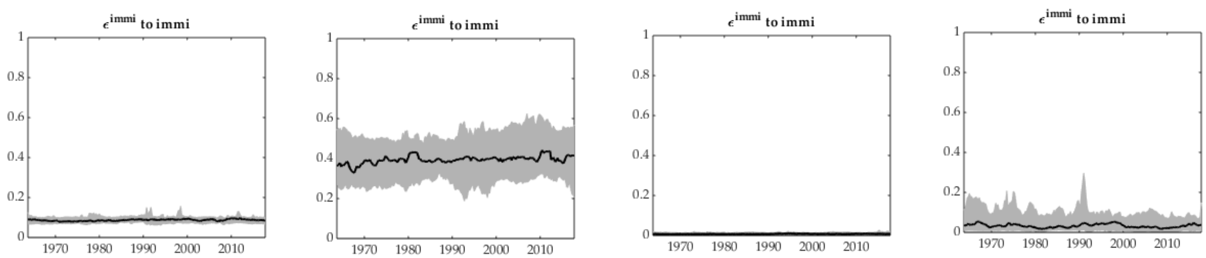

(c) Forecast Horizon: 20 Quarters

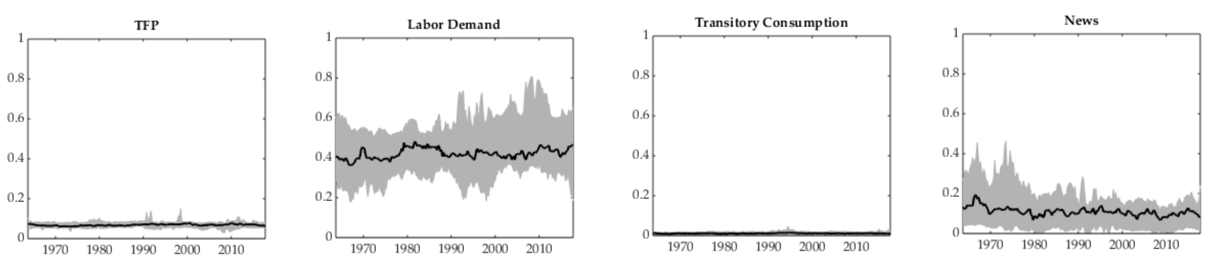

(d) Forecast Horizon: 32 Quarters

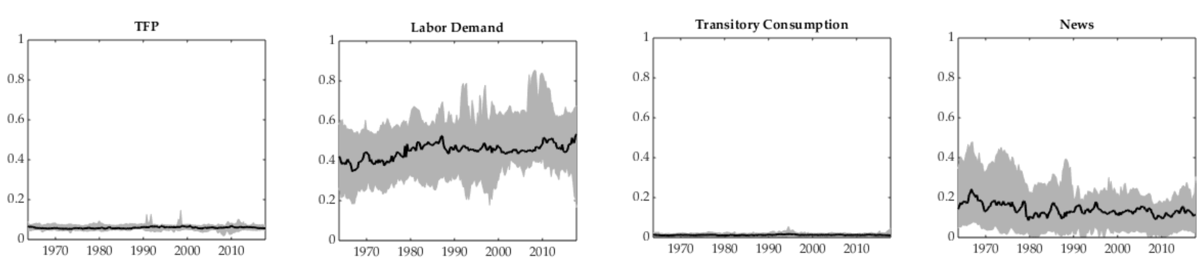

Notes: The solid (black) lines are median values of forecast error variance decompositions at 4, 8, 20, and 32 quarters after initial shock. Gray shaded areas are 16-84% posterior tunnels. SVAR estimated with Model 1.

Fig. I.12. Posterior Estimates of Impact TVPs, Estimated with Model 1, 1963Q1 - 2017Q4

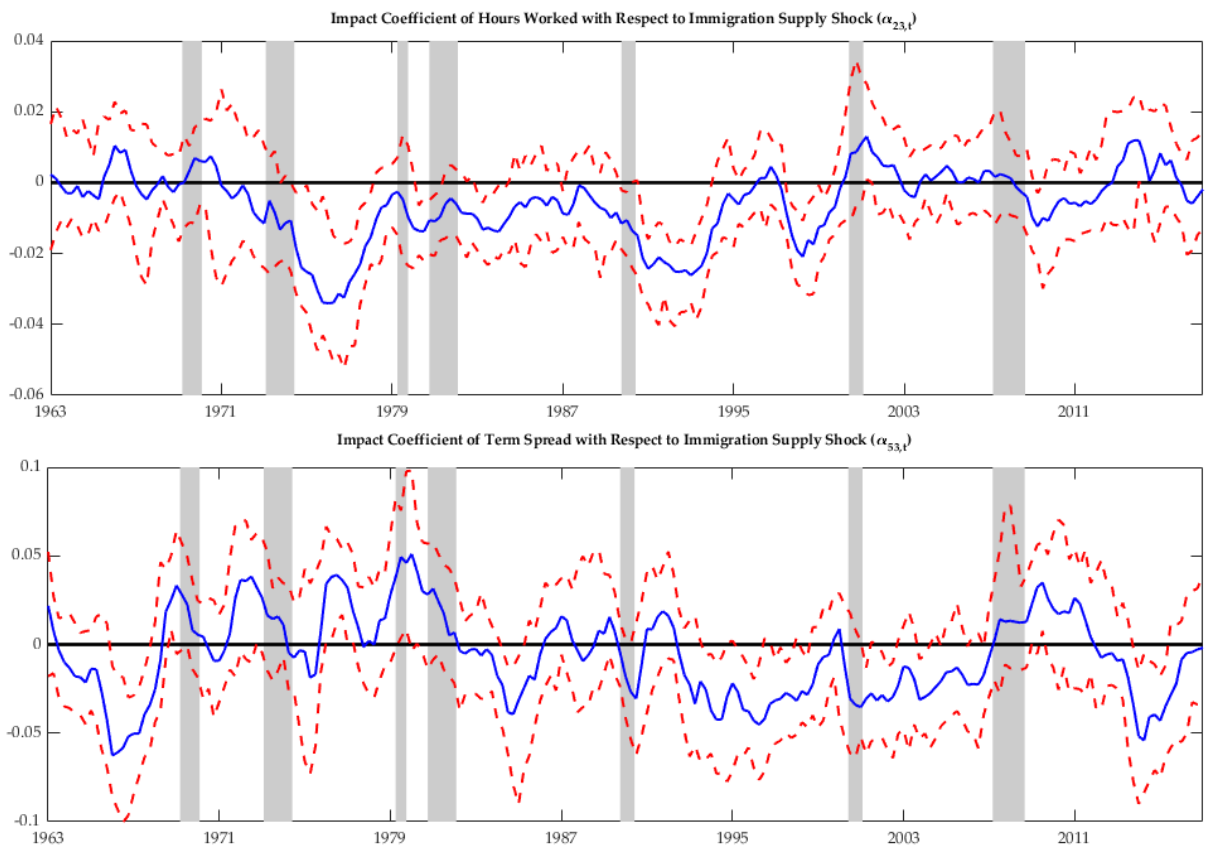

Notes: Median values of the posterior estimates of impact coefficients are solid (blue) lines. The dotted (red) lines are 16-84 percent bands. The sample period is 1963Q1 to 2017Q4. X-axis: sample date; y-axis: magnitude of estimate. Gray shades are NBER recession trough dates.

Fig. I.13. Posterior Estimates of Impact TVPs, Estimated with Model 1, 1963Q1 - 2017Q4

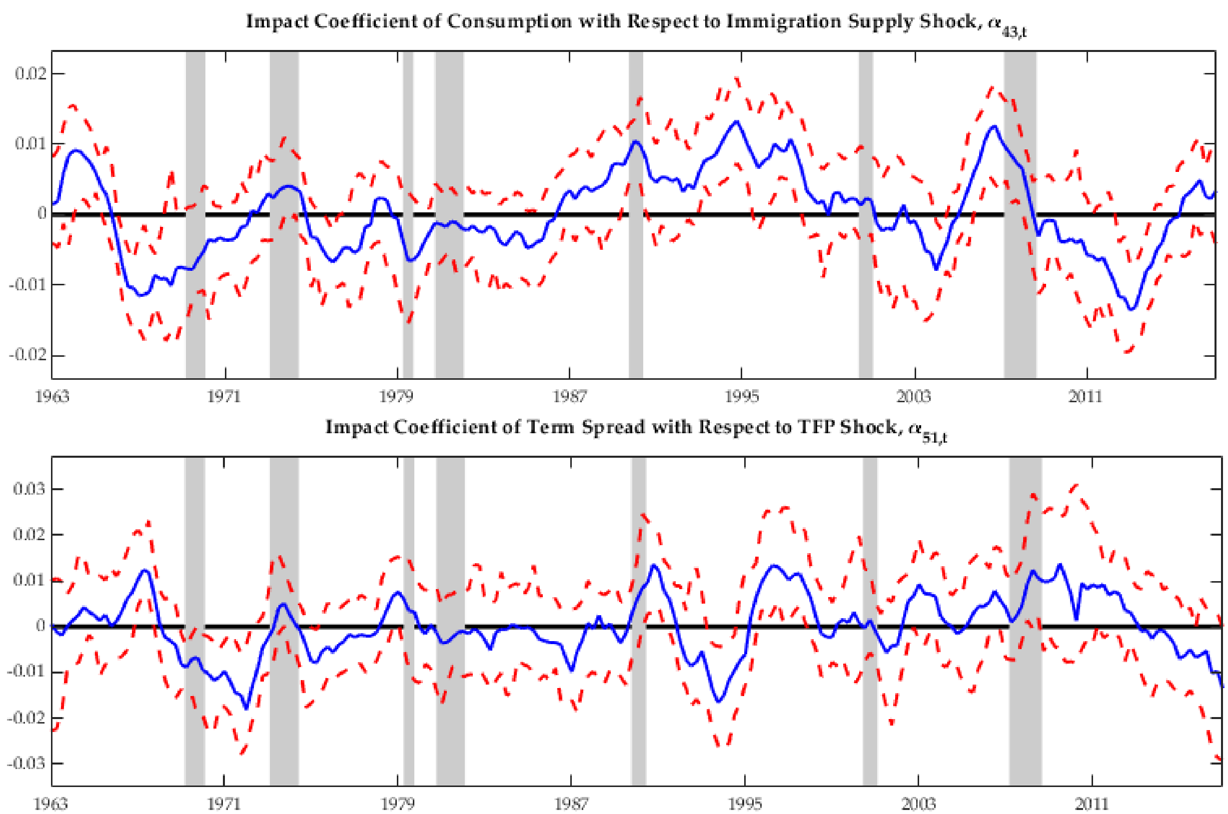

Notes: Median values of the posterior estimates of impact coefficients are solid (blue) lines. The dotted (red) lines are 16-84 percent bands. The sample period is 1963Q1 to 2017Q4. X-axis: sample date; y-axis: magnitude of estimate. Gray shades are NBER recession trough dates.

I.2. Robustness Check on Annual Versus Quarterly Data

To answer an anonymous reviewer's request, I present IRFs of fixed parameters SVARs identified with $A^{I}_{0,t}$ and $\tilde{D}^{II}_{t}$ (Model 13) estimated with annual data and with quarterly interpolated data as the main text. Panel (a) of Figure I.14 shows the IRF of ALP with respect to an immigration supply shock. Panel (b) shows the IRF of immigration with respect to a news shock. The IRFs estimated with annual data and those estimated with quarterly data display qualitatively and quantitatively similar responses.

Fig. I.14. IRFs of Fixed Parameter SVAR, Annual Data Versus Quarterly Data

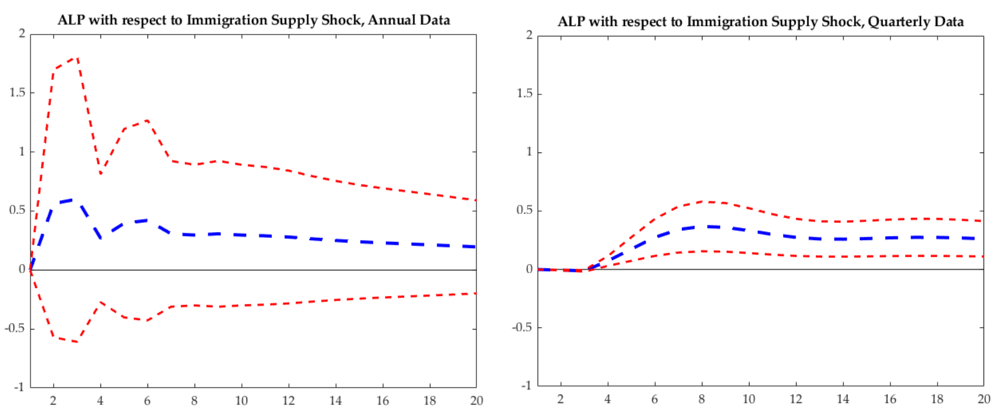

(a) Average Labor Productivity with respect to an Immigration Supply Shock

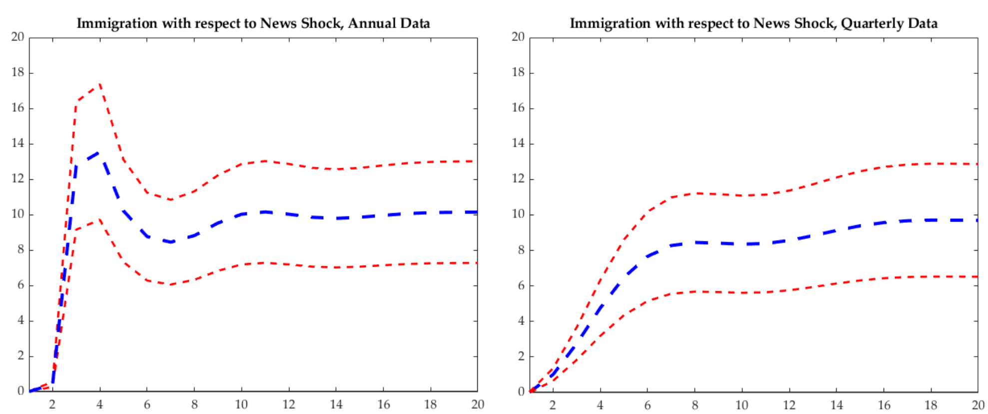

(b) Immigration with respect to a News Shock

Notes: The left panels show IRFs estimated with annual data. The right panels show IRFs estimated with quarterly data. Median responses (in blue) and 16-84% error bands (in red). Sample is 1953 to 2017.

References

Baker, S. G. (1997). The “amnesty” aftermath: Current policy issues stemming from the legalization programs of the 1986 immigration reform and control act. *International Migration Review*, 31(1):5.

Basu, S., Fernald, J., and Kimball, M. (2006). Are technology improvements contractionary? *American Economic Review*, 96(5):1418–1448.

Beaudry, P., Feve, P., Guay, A., and Portier, F. (2019). When is nonfundamentalness in SVARs a real problem? *Review of Economic Dynamics*, 34:221–243.

Beaudry, P. and Portier, F. (2014). News driven business cycles: Insights and challenges. *Journal of Economic Literature*, 52(4).

Benson, O. G. (2016). Refugee resettlement policy in an era of neo–liberalization: A policy discourse analysis of the refugee act of 1980. *Social Service Review*, 90(3):515–549.

Borjas, G. (1994). The economics of immigration. *Journal of Economic Literature*, 32:1667–1717.

Canova, F. and Perez-Forero, F. J. (2015). Estimating overidentified, nonrecursive, time-varying coefficients structural vector autoregressions. *Quantitative Economics*, 6(2):359–384.

Carter, C. K. and Kohn, R. (1994). On Gibbs sampling for state space models. *Biometrika*, 81(3).

Chow, G. C. and Lin, A.-L. (1971). Best linear unbiased interpolation, distribution, and extrapolation of time series by related series. *The Review of Economics and Statistics*, 53(4):372.

Cociuba, S. E., Prescott, E. C., and Ueberfeldt, A. (2018). US hours at work. *Economics Letters*, 169:87–90.

Correa-Cabrera, G. and Rojas-Arenaza, M. (2012). The mathematics of Mexico-US migration and US immigration policy. *Policy Studies*, 33(4):297–312.

Fisher, I. (1922). *The making of index numbers, study of their varieties, tests, and reliability*. Houghton Mifflin.

Forni, M. and Gambetti, L. (2014). Sufficient information in structural VARs. *Journal of Monetary Economics*, 66:124–136.

Forni, M., Gambetti, L., and Luca, S. (2014). No news in business cycles. *Economic Journal*, 124:1168–1191.

Forni, M., Gambetti, L., and Sala, L. (2019). Structural VARs and noninvertible macroeconomic models. *Journal of Applied Econometrics*, 34(2):221–246.

Friedberg, R. M. and Hunt, J. (1995). The impact of immigrants on host country wages, employment and growth. *Journal of Economic Perspectives*, 9(2):23–44.

Galí, J. (1999). Technology, employment, and the business cycle: Do technology shocks explain aggregate fluctuations? *American Economic Review*, 89(1):249–271.

Geweke, J. (1999). Using simulation methods for Bayesian econometric models: inference, development and communication. *Econometric Reviews*, 18(1):1–73.

Geweke, J. (2005). *Contemporary Bayesian Econometrics and Statistics*. Wiley & Sons, Inc.

Hanson, G. and Splimbergo, A. (2001). Political economy, sectoral shocks, and border enforcement. *Canadian Journal of Economics*, 34(3).

Law, A. O. (2002). The diversity visa lottery: A cycle of unintended consequences in United States immigration policy. *Journal of American Ethnic History*, 21(4):329.

Lucas, R. E. (1975). The supply-of-immigrants function and taxation of immigrants incomes. *Journal of Development Economics*, 2(3):289–308.

Omori, Y., Chib, S., Shephard, N., and Nakajima, J. (2007). Stochastic volatility with leverage: Fast and efficient likelihood inference. *Journal of Econometrics*, 140(2):425–449.

Orrenius, P. M. and Zavodny, M. (2003). Do amnesty programs reduce undocumented immigration? Evidence from IRCA. *Demography*, 40(3):437.

Primiceri, G. E. (2005). Time varying structural vector autoregressions and monetary policy. *The Review of Economic Studies*, 72(3):821–852.

Rothenberg, T. J. (1971). Identification in parametric models. *Econometrica*, 39(3):577.

Rubio-Ramirez, J. F., Waggoner, D. F., and Zha, T. A. (2010). Structural vector autoregressions: Theory of identification and algorithms for inference. *Review of Economic Studies*, 77:665–696.

Silva, J. S. and Cardoso, F. (2001). The Chow-Lin method using dynamic models. *Economic Modelling*, 18(2):269–280.

Vernez, G. (1993). The United States immigration reform and control act of 1986: Implementation and effects. *Migration Policies in Europe and the United States*, pages 83–96.

Whelan, K. (2002). A guide to the use of chain aggregated NIPA. *The Review of Income and Wealth*, 48(2):217–233.